ELSEVIER

Journal of Alloys and Compounds 293–295 (1999) 626–631

Journal of ALLOYS AND COMPOUNDS

Charge and discharge characteristics of sintered Mg_2Ni

Kuniaki Watanabe*, Wei Min Shu, Kenzo Mizukami, Kohji Kobayashi, Yuji Hatano, Shotaro Morozumi

Hydrogen Isotope Research Centre, Toyama University, Gofuku 3190, Toyama 930-8555, Japan

Abstract

The effects of sample preparation of a Mg_2Ni anode for a nickel/metal hydride battery were studied with an open electrochemical cell. The discharge capacity of sintered Mg_2Ni increased initially with the charge/discharge cycles. The cycle life (CL) for sintered samples was much greater than that of un-sintered samples, and the largest CL appeared at a sintering temperature of 550°C. It was also observed that slight pre-oxidation of the sample powder was effective in improving the CL.

Those effects were examined through the changes in the specific surface area and the chemical composition. The sample sintered at 550°C had the largest specific surface area, and the segregation of Mg over the outside layer of samples was confirmed for those sintered at temperatures higher than 550°C. The degradation after charge/discharge cycling was investigated with X-ray diffraction and scanning electron microscopy. The XRD pattern showed a new phase of $Mg(OH)_2$, besides the phase of Mg_2Ni, after charge/discharge cycling. This indicates that the formation of $Mg(OH)_2$ on the outside layer of the samples contributes to the degradation of the anode performance.

Keywords: Hydride; Battery; Mg_2Ni; Cycle-life; Pretreatment

1. Introduction

Magnesium and magnesium-based alloys are known to have much higher hydrogen absorbability than conventional hydrogen storage alloys such as AB_5 and AB_2 types, in addition to their lower specific gravity and richer natural resources [1–5]. It has been recognized, however, that magnesium and magnesium-based alloys need to be operated at much higher temperatures because of their lower equilibrium pressure and poor surface activity [4,5].

It was recently found that some amorphous Mg–Ni alloys prepared by mechanical alloying can adsorb and desorb electrochemically a large amount of hydrogen at room temperature [6]. This makes it a very promising material for Ni–metal hydride rechargeable batteries. Similar features could be expected for crystalline Mg_2Ni. However, electrode properties are very much dependent on its preparation procedures which affect the pore structure, the aggregation state of the crystallite particles, the surface chemical state and so on. For example, Lei et al. observed serious oxidation of magnesium and nickel for amorphous Mg–Ni [6,7]. This is considered to be the reason for its much faster degradation in discharge capacity than that of AB_5, AB_2 and AB-type metal hydride electrodes.

In this work, Mg_2Ni electrode was prepared under various sintering conditions, as a new anode preparation technique. The sintered Mg_2Ni without any binder was electrochemically characterized in order to evaluate briefly its possibility as anode material in nickel–metal hydride batteries. The present paper describes the effects of sintering temperature and pre-oxidation treatment on the hydride anode performance along with the measurements of specific surface area, chemical composition, X-ray diffraction and scanning electron microscopy.

2. Experimental

In the Mg–Ni system, there are two intermetallic compounds, Mg_2Ni and $MgNi_2$. The latter does not react with hydrogen, at least up to temperatures of 350°C and pressures of 2.8 MPa, whereas the former reacts readily with hydrogen at 325°C and 2.1 MPa, producing a ternary hydride with the formula of Mg_2NiH_4[4,5]. The material used in this study was Mg_2Ni powder (below 200 mesh) purchased from Japan Metals & Chemicals. Three types of samples were prepared in order to investigate the effects of sample preparation. Sample 1 (0.2 g) was first pressed into a disk of 10 mm in diameter and 1 mm in thickness by using a force of 40 MPa, then sintered in an argon

*Corresponding author.

0925-8388/99/$ – see front matter
PII: S0925-8388(99)00355-2

atmosphere at varying temperatures from 450 to 625°C, and finally sandwiched between nickel meshes as a current collector. Sample 2 (0.5 g), on the other hand, was first pressed into a rectangle of 15×20 mm on a nickel mesh, and then sintered in an argon atmosphere at temperatures from 450 to 625°C. Sample 3 (0.5 g) was prepared to observe effects of pre-oxidation by which a more firm electrode could be obtained. Namely, the sample powder was first oxidized in air at 200°C for varying periods of time, pressed on a nickel mesh and then sintered at 550°C in Ar flow.

Electrochemical measurements were conducted at room temperature by use of a nickel–hydrogen battery test device comprised of a battery charge/discharge unit (Hokuto Denko, HJ-201B). The test cell was filled with 6 M KOH electrolyte solution. The test cathode was $NiOOH/Ni(OH)_2$, and the anode was sample 1, 2 or 3, where the total capacity of the cathode was much larger than that of the anode. The discharge capacity of the anode was expressed in mAh per gram of the alloy. Sample 1 was charged at 20 mA for 10 min, then rested for 10 min, and discharged at 5 mA. For samples 2 and 3, on the other hand, the charge was set at 40 mA for 30 min, rest for 10 min, and discharge at 10 mA.

The apparatus to determine specific surface area consisted of a vacuum pumping system, a gas supply system, a sample tube, a handmade ohmic heater and a measuring system. The residual pressure of the vacuum system was usually below 10^{-6} Pa. The reaction volume was calibrated by gas expansion. Prior to measurements, the sample was activated at 150°C for 2 h by a temperature programmer connected to the heater. The surface areas were measured at liquid nitrogen temperature with krypton following the BET method.

The chemical composition was measured by an energy dispersion spectrometer (EDS, EDAX 9100) and a X-ray spectrometer (XRS, Philips PW2300). The Mg content of the outside of the electrode samples was measured by EDS. After the EDS measurement, the samples were pulverized mechanically into powder, and then the Mg content in the inner part of the sample electrode was measured by XRS.

The crystallographic features of samples before and after charge/discharge cycles were measured by X-ray diffraction (XRD, Philips PW1700). Powder morphology was observed by scanning electron microscopy (SEM, EDAX 9100) before and after charge/discharge cycles.

3. Results and discussion

3.1. Cycle life of sintered electrodes

Mg_2Ni electrochemically absorbs and desorbs hydrogen in alkaline solution as a reversible anode. The overall reaction is written as

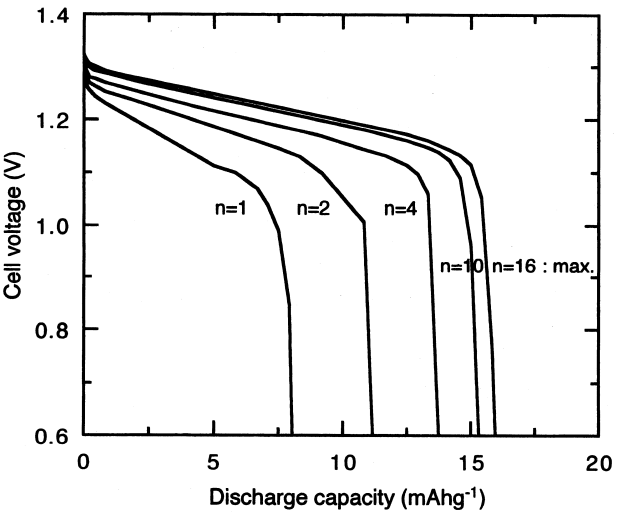

Fig. 1. Discharge curves of sample 1 sintered at 475°C for cycle numbers of 1, 2, 4, 10 and 16.

$$Mg_2Ni + 4Ni(OH)_2 \rightleftharpoons Mg_2NiH_4 + 4NiOOH.$$

Fig. 1 shows typical discharge curves, which were measured for sample 1 sintered at 475°C. It can be seen in the figure that the discharge capacity increased initially with the cycle number. This suggests that the activation of alloy surfaces took place during the initial charge/discharge cycling. The maximum capacity appeared at cycle number of 16 for this sample. Both samples 1 and 2 were sintered in Ar atmosphere at varying temperatures. Fig. 2 shows discharge characteristics of sample 1 sintered at various temperatures. The axis of coordinate is DE (Discharge Efficiency), i.e. the fraction of discharged capacity to charged capacity. A cycle life (CL) was defined here as cycle numbers at which the discharged capacity decreased to one half of charged capacity. As shown in Fig. 2, CL for sintered samples was much greater than that of the un-

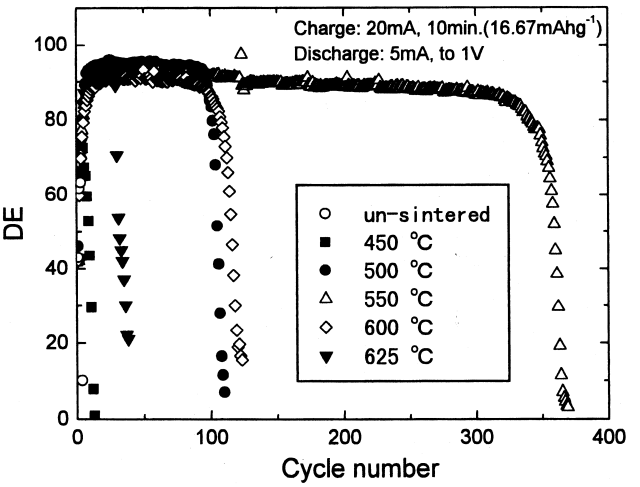

Fig. 2. Discharge characteristics of sample 1 for un-sintered and sintered at various temperatures.

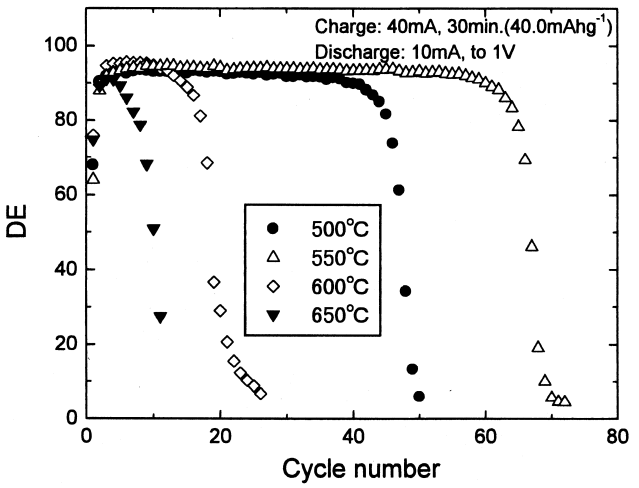

Fig. 3. Discharge characteristics of sample 2 sintered at 500, 550, 600 and 650°C.

sintered sample, and the largest CL (about 350) appeared at the sintering temperature of 550°C. In other words, CL increased initially with elevating sintering temperature below 550°C, and then decreased with sintering temperature above 550°C.

For sample 2, the discharge characteristics are shown in Fig. 3 for the sintering temperatures of 500, 550, 600 and 650°C. Similarly, the largest CL appeared at the sintering temperature of 550°C. This is clearly seen in Fig. 4, where the CL's for the two types of samples are plotted together against sintering temperature. For both of the samples, 1 and 2, the largest CL appeared at the sintering temperature of 550°C. However, the CL of sample 2 was smaller than that of sample 1 at the same sintering temperatures. This appears partly due to different charge/discharge conditions between the two. Namely, it is considered that the CL for sample 2 would be much larger than that of sample 1 if the charge and discharge conditions were the same for the two types of samples, considering that the charged capacity of sample 2 was a few times greater than that of sample 1, and that discharged current for sample 2 was double of that for sample 1.

3.2. Cycle life of pre-oxidized electrode

It was found that much firmer electrodes could be prepared by pre-treatment of the powder, such as by oxidation in the air. This was expected to be effective for avoiding the peeling-off of the electrode, which was observed for samples 1 and 2 sintered at low temperatures, during the charge and discharge cycles. The charge and discharge properties were measured for the pre-oxidized anode, sample 3, under the same conditions as sample 2.

Fig. 5 shows the effect of pre-oxidation treatment on CL, where the sample powder was oxidized in the air at 200°C for the given times, and subsequently was pressed on a nickel mesh and then sintered at 550°C. It can be seen that the oxidation initially improved CL with increasing oxidation time. However, longer oxidation over 20 min resulted in reduced improvement.

Another characteristic feature is the descending slope of DE with increasing cycle number in the region where it was kept almost constant for samples 1 and 2. However, a similar feature was also observed for the un-oxidized electrode in these runs. Therefore, it cannot be ascribed to the pre-oxidation treatment. Reasons for this difference between the un-oxidized and oxidized samples are not clear yet, but it is presumably due to the different lots of sample powder.

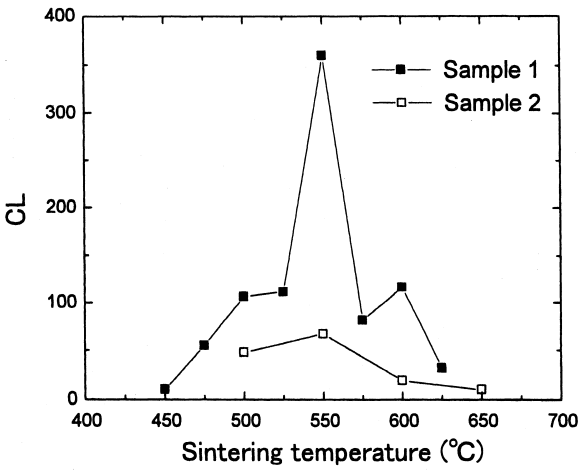

Fig. 4. Dependence of the cycle life on sintering temperature for two types of samples.

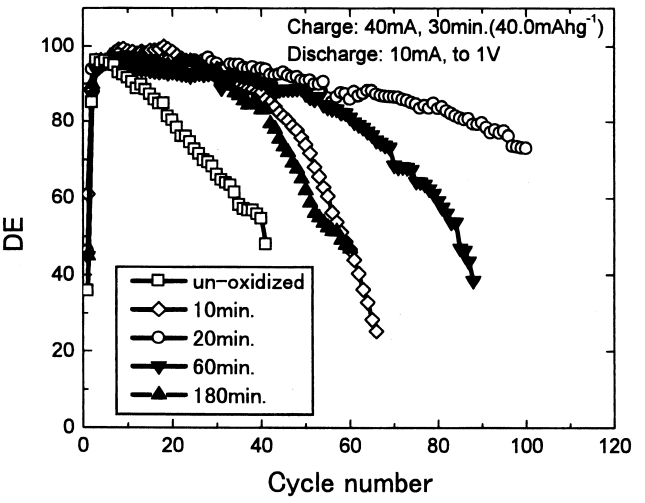

Fig. 5. Effect of pre-oxidation treatment on discharge characteristics of sample 2.

3.3. Changes in surface area and chemical composition with sintering

As shown in Fig. 4, CL's of both samples 1 and 2 sintered below 550°C were smaller than those sintered at 550°C, and those above 550°C were also smaller. At temperatures lower than 550°C, the binding between fine powder was so weak that some powder peeled off after a few cycles of charge and discharge. This appears to be the predominant reason for smaller CL's of the samples sintered at low temperatures. On the other hand, the degradation above 550°C cannot ascribed to insufficient sintering nor surface poisoning owing to impurity gases in Ar gas at high temperature sintering.

The degradation of the anode performance for the samples sintered at higher temperatures was then examined through the measurement of specific surface area and the analysis of chemical compositions. The specific surface areas determined by the BET method are shown in Fig. 6 for the un-sintered sample (dashed line) and those sintered at 500, 550 and 600°C. The specific surface area sintered at 500°C was a little larger than that of the un-sintered sample, and a maximum appeared at 550°C. For the sample sintered at 600°C, however, the specific surface area was even smaller than that of the un-sintered sample. The decrease in specific surface area appears to be one of the reasons of the CL degradation for the samples sintered at temperatures higher than 550°C.

The chemical compositions were measured by both EDS (the outside of the sample electrode) and XRS (the inside of the electrode). Changes in Mg content of sintered samples to the un-sintered sample are plotted in Fig. 7 against sintering temperature. The X-ray spectrometer results show that the inside Mg-content drops by about 7 to 12 at% for sintered samples compared with the un-sintered one. The EDS results, however, show that the outside Mg-content was larger for sintered sample than for the un-sintered, except the sample sintered at 500°C. Especially, the sample sintered at 650°C shows Mg enrichment by about 8 at% at the outside layer. The Mg segregation at the outside layer possibly contributes to the CL degradation of the samples sintered at temperatures higher than 550°C.

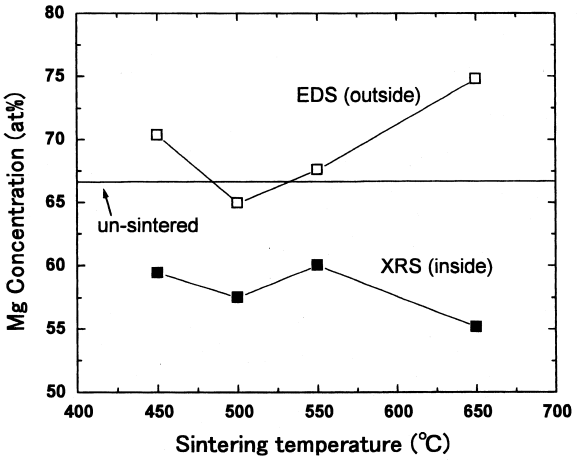

Fig. 7. Variation in Mg concentration with sintering temperature.

3.4. Changes in crystallographic and morphological natures with cycling

The degradation with charge/discharge cycling was investigated by XRD and SEM for the samples before and after cycling. Fig. 8 shows the XRD results of sample 2 sintered at 550°C. The as-prepared sample was pulverized mechanically into powder after sintering and then the powder was measured by XRD. Similarly, the sample after

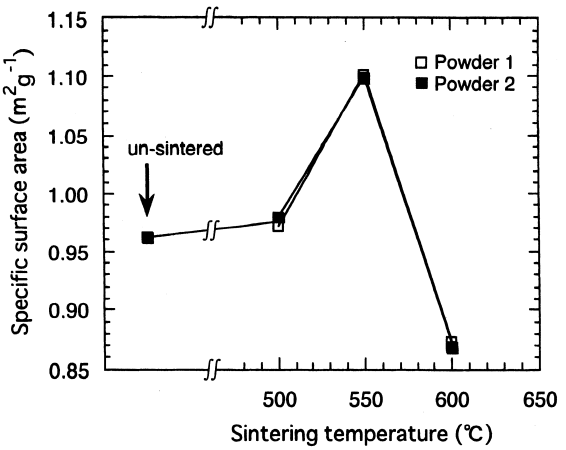

Fig. 6. Specific surface areas for samples un-sintered and sintered at 500, 550 and 600°C.

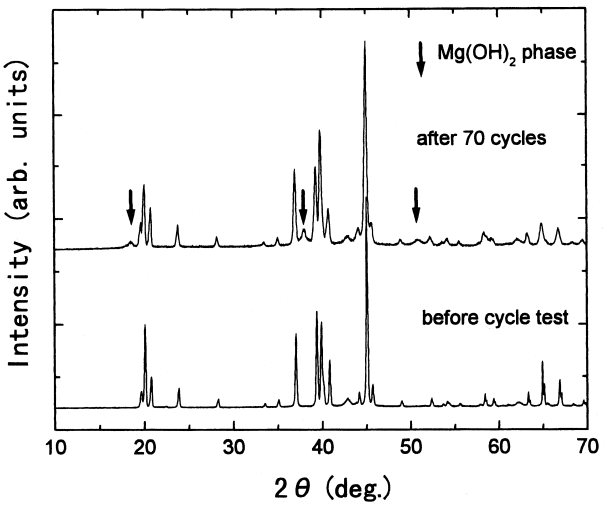

Fig. 8. XRD diagrams before and after charge/discharge cycling for sample 2 sintered at 550°C.

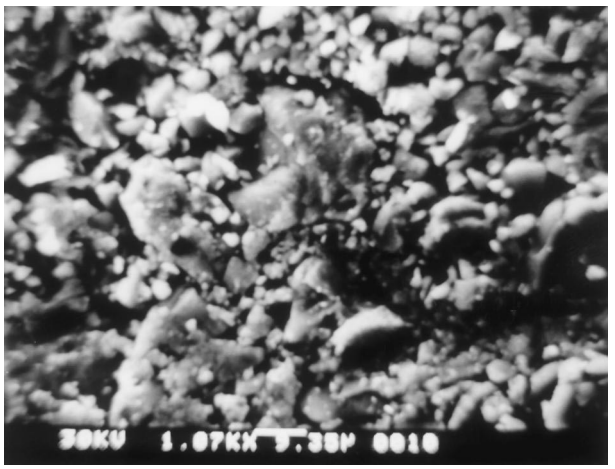

Fig. 9. SEM morphology of sample 2 before charge/discharge cycling.

cycling was pulverized mechanically into powder after 70 cycles for XRD measurement. The XRD results indicates that a single phase of Mg_2Ni exists in the as-prepared sample while there appears a new phase of $Mg(OH)_2$ besides the phase of Mg_2Ni in the sample of after charge/discharge cycling.

SEM morphology of sample 2 before and after charge/discharge cycling is shown in Figs. 9 and 10. The powder particles on the outside of the sample before charge/discharge cycling have definite boundaries, while those after the cycle test became a little vague. This difference may be attributed to the formation of $Mg(OH)_2$ during the charge/discharge cycling. It is well-known that the hydrogen absorbing and desorbing cycles bring about the pulverization of the alloy, continuously enlarged surface area, production of fresh surface and the formation of oxide or hydroxide. Therefore, the repeated charging and discharging in KOH solution caused continuous degradation of the alloy. The hydrogen storage capacity of a $LaNi_5$ anode was reduced to as much as 40% of the initial value after only 100 charge/discharge cycles due to the decomposition of $LaNi_5$ to $La(OH)_3$ and Ni [8]. Willems et al.[9] have found that the anodes of $LaNi_{2.5}Co_{2.5}$-based alloys have a much longer cycle life than $LaNi_5$ or its ternary alloys, though the replacement of Ni by Co brought about a considerable decrease in the hydrogen storage capacity. They argued that the significant improvement of durability was closely associated with the reduction of volume expansion ratio of the alloy to its hydride [9]. Sakai et al. [10,11] have reported that the surface coating of pulverized $LaNi_5$ by porous copper or nickel was very useful for increasing the cycle life, because the coated metal film works as both an oxidation barrier to protect the metal hydride and a micro current collector for proceeding electrochemical reactions on the surface.

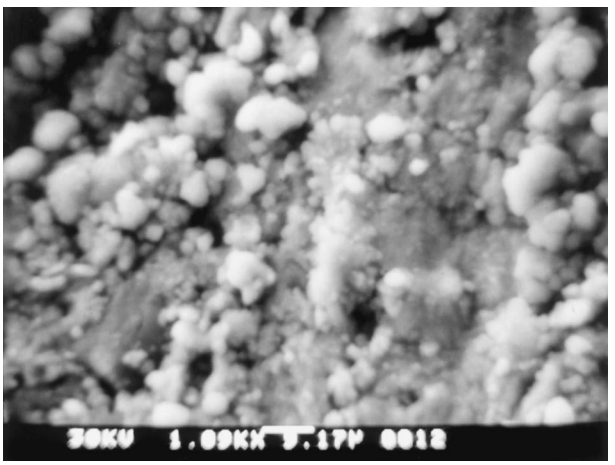

Fig. 10. SEM morphology of sample 2 after charge/discharge cycling.

It is thus deduced that the charge/discharge characteristics of the Mg_2Ni anode are very sensitive to the aggregation between fine powder particles, accumulation of hydrogen and $Mg(OH)_2$ in/on the anode, and so on, resulting in a change in conductivity, and is expected to be much improved by solving these problems.

4. Conclusions

The charge/discharge cycling experiments showed that sintered and pre-oxidized Mg_2Ni is a promising anode material. The results of the present study are summarized as the following:

1. The discharge capacity increased initially with the cycle number, indicating that the activation of the anode surface occurs during the initial charge/discharge cycling.
2. The cycle life (CL) of Mg_2Ni anode could be much improved by sintering as well as pre-oxidation treatment.
3. The largest CL appeared at the sintering temperature of 550°C. At temperatures lower than 550°C, the weak binding between the fine powders is the main reason for the small CL. At temperatures higher than 550°C, the decrease in specific surface area and Mg segregation at the outside layer contribute to the CL degradation for the samples sintered. As to the slight pre-oxidation, firm aggregation between Mg_2Ni powder appears to play a role in the improvement.
4. A new phase of $Mg(OH)_2$ appeared after charge/discharge cycling, besides the original phase of Mg_2Ni. It suggests that the $Mg(OH)_2$ phase on the outside layer of the samples degrades the anode performance.

5. Acknowledgment

This work has been supported in part by a Grand-in-Aid for Scientific Research on Priority Areas A of ‘‘New

Protium Function'' from the Ministry of Education, Science, Sports and Culture.

The authors are also indebted to Dr. K. Matsuda (Faculty of Engineering, Toyama University) for operating the SEM/EDS instruments. They are also grateful for a gift of the cathode material from Human Environmental Systems Development Center of National/Panasonic Co. and for that of the anode alloy from Japan Metals and Chemicals Co.

References

[1] J.J. Reilly, R.H. Wiswall Jr., Inorg. Chem. 7 (1968) 2254.
[2] Z. Gavra, M.H. Mintz, G. Kimmel, Z. Hadari, Inorg. Chem. 18 (1979) 3595.
[3] J. Genossar, P.S. Rudman, J. Phys. Chem. Solids 42 (1981) 611.
[4] D. Noreus, K. Jansson, M. Nygren, Z. Phys. Chem. 146 (1985) 191.
[5] D. Noreus, L. Kihborg, J. Less-Common Met. 123 (1986) 233.
[6] Y.Q. Lei, Y.M. Wu, Q.M. Yang, J. Wu, Q.D. Wang, Z. Phys. Chem. 183 (1994) 379.
[7] D.L. Sun, Y.Q. Lei, W. Liu, J.J. Jiang, J. Wu, Q.D. Wang, J. Alloys and Compounds 231 (1995) 621.
[8] T. Sakai, H. Ishikawa, H. Miyamura, N. Kuriyama, J. Electrochem. Soc. 138 (1991) 908.
[9] J.J.G. Willems, K.H.J. Buschow, J. Less-Common Met. 129 (1987) 13.
[10] T. Sakai, K. Ishikawa, K. Oguro, C. Iwakura, H. Yoneyama, J. Electrochem. Soc. 134 (1987) 558.
[11] C. Iwakura, Y. Kajiya, H. Yoneyama, T. Sakai, K. Oguro, H. Ishikawa, J. Electrochem. Soc. 136 (1989) 1351.